March 1989

CRACK ARREST REQUIREMENTS FOR ARCTIC STRUCTURES

Final Report
by

B.A.Graville

Work on this project was conducted under the auspices of the Department of Energy, Mines and Resources

DSS FILE NUMBER: 009SQ.23440-8-9190

DSS CONTRACT NUMBER: 23440-8-9190/01-SQ

EMR SCIENTIFIC AUTHORITY: Dr. W.R. Tyson

44 pp

GRAVILLE ASSOCIATES INC.

P.O.Box 225 Georgetown Ontario L7G 4Y5 Tel: (416) 873-1739 FAX: (416) 873-0466

MICROMEDIA

CONTENTS

Executive summary ..... ii)

Introduction ..... 1)
Review of the Fracture Analysis Diagram ..... 3)
Review of Crack Arrest Data ..... 6)
- Test Types ..... 6)
- Analysis ..... 6)
- Analysis of Scatter ..... 8)
- Effect of Thickness ..... 8)
- Effect of Test Type ..... 9)

Analysis of CSA S473 Requirements ..... 11)
- Moderate Crack Arrest Capability ..... 11)
- Good Crack Arrest ..... 13)

General Discussion and Conclusions ..... 16)
References ..... 17)
Tables ..... 20)
Figures ..... 31)
Appendix A ..... 40)

EXECUTIVE SUMMARY

Crack arrest performance of modern Arctic-grade steels have been reviewed in the context of the currently proposed toughness requirements for offshore structures contained in CSA Preliminary Standard S473. The results confirm that the drop weight test is better than the Charpy test for specifying steel based on crack arrest behaviour. The nil-ductility transition temperature (NDTT) correlates quite well with results of compact crack arrest tests and dynamic crack initiation tests, but there is considerable variation in the relation between crack arrest toughness measured by double tension temperature gradient tests and the NDTT. The results show that for the majority of data reviewed the current CSA S473 requirements are conservative. Low values of crack arrest toughness could not be associated with any particular aspect of the steel, but high values may be promoted by splitting behaviour which can be pronounced in thermo-mechanically controlled processed steels. An alternate criterion for moderate crack arrest based on a constant plane strain crack tolerance is proposed for redundant members. Because of the wide scatter in crack arrest properties it is recommended that crack arrest data be obtained on a case-by-case basis for steels used in fracture critical members.

Crack Arrest Requirements for Arctic Structures

Introduction

A significant aspect of Preliminary Standard CSA S473 (Code for the Design, Construction, and Installation of Fixed Offshore Structures, Part III - Steel Structures), and one which affects both the safety and economy of offshore structures is the material toughness requirements. Most toughness requirements for critical structures in North America (1) have their origin in the Fracture Analysis Diagram (FAD) developed by Pellini et al during the 1950's and which was derived from extensive research on fractures in ship plates. The Fracture Analysis Diagram (Fig. 1) defines the stress and temperature conditions necessary for dynamic fracture initiation or crack arrest and is indexed by the single point Nil Ductility Transition Temperature (NDTT). The NDTT is readily determined for a material using the drop weight test as described in ASTM E208 (2). In most specifications, material toughness is specified in terms of Charpy V Notch (CVN) properties through correlations with the NDTT or more directly with service experience.

CSA S473 takes a similar approach but with some important differences. First, the Standard provides for a range of toughness levels according to the structural member classification ('box' number) based on risk of fracture initiation and consequences of fracture. This provides the designer flexibility in material selection and avoids overspecifying materials for non-critical applications. Second, toughness is specified directly in terms of drop weight test requirements supplemented by CVN tests. This was thought necessary because recent evidence (3) shows that correlations between CVN and drop weight test results are unreliable for modern very clean steels. For the base metal, CSA S473 sets three levels of toughness denoted as: 'none,' 'moderate,' and 'good' crack arrest ability. The corresponding NDTT requirements (Table 1) are derived from a recent version of the Fracture Analysis Diagram which includes the effect of thickness.

The Fracture Analysis Diagram and consequently the CSA S473 requirements use a temperature shift approach. That is, the toughness test temperature is set at a value displaced from the minimum design temperature by an amount determined from the Fracture Analysis Diagram depending upon the fracture criteria adopted. Temperature shift methods have been widely used in material specifications because they allow the steel toughness to be

specified in terms of simple tests such as the Charpy. This method assumes a constant change in toughness with temperature for all materials such that the shape of the Fracture Analysis Diagram is material independent. This, however, is not necessarily true, although such a simplifying assumption is appealing for the purposes of writing a minimum standard.

The approach taken in CSA S473, and inherent in the FAD, is that the crack arrest properties can be established from a knowledge of the NDTT. In order to validate the CSA S473 approach, the present work was undertaken to review crack arrest data from modern arctic grade steels in terms of the NDTT (denoted NDT in earlier references) and the Fracture Analysis Diagram.

Review of the Fracture Analysis Diagram

The Fracture Analysis Diagram had its origin in extensive research on ship plates following World War II. It was learned that brittle fracture in low and medium strength steels was associated with brittle initiation. At some point in the structure a brittle region, such as a tack weld or an arc strike, cracked initiating a brittle fracture which was followed by crack propagation. Brittle initiation was simulated in the drop weight test which determines the Nil Ductility Transition Temperature (NDTT). The NDTT is the highest temperature at which a small running crack continues to propagate across the specimen when loaded to the dynamic yield stress of the material. With the NDTT as a reference index, the Fracture Analysis Diagram plots the fracture strength/temperature transition behaviour. The limiting case (the lower and right hand curve in the FAD) is the crack arrest curve beyond which a brittle fracture cannot be sustained in the material. The crack arrest curve in the original FAD was defined from Robertson crack arrest tests.

The original FAD including the crack arrest curve was independent of material thickness and was considered valid for thicknesses up to about 1 in. The need for very thick walled vessels in nuclear applications stimulated extensive work on thickness effects during the 60' and 70's. As a consequence, a revised Fracture Analysis Diagram was proposed(4) which included a crack arrest curve for very thick sections which was expanded to the right of the original curve (Fig. 2). Because of the very high cost involved in establishing crack arrest curves, Pellini subsequently proposed (5) an alternate method of deriving the position of the crack arrest curve. Recognizing that the crack arrest curve corresponded to a stress state transition in which elastic-plastic fracture took place, he proposed a method of defining this transition on the basis of fracture mechanics. The beginning of rapid rise in toughness was associated with loss of plane strain conditions and was expected to occur at the point where the dynamic fracture toughness K_{Id} was given by

$$K_{Id} = 0.63\ \sigma_{yd}\sqrt{t}$$

where σ_{yd} is the dynamic yield strength and t, the thickness.

Similarly, the top part of the crack arrest curve, where a nominal stress equal to the yield stress was required to propagate a crack, would be where the plane strain fracture toughness was about

$$K_{Id} = 1.0\ \sigma_{yd}\sqrt{t}$$

Pellini believed these criteria to be quite conservative. The position of these two index points denoted respectively as *L* and *YC*, could be found from the dynamic toughness K_{Id} curve. Pellini considered the ASTM curve too conservative and proposed his own reference toughness curve. As a design guide (6) for conventional structural low and medium strength steels, a constant value of the dynamic yield strength of 487 MPa (70 ksi) was assumed, and this resulted in the diagram shown in Fig. 3 which was used in developing the CSA S473 toughness requirements.

It is important to note that although the Pellini diagram shows stress against temperature, stress is not used in calculating the position of the *L* point. *L* defines the limit of plane strain capacity, and therefore represents a limit on crack tip stress intensity factor. In early papers (5) the *L* point was set at 0.3 σ_y. This figure can be rationalized by considering the smallest through-thickness crack (of half-length *a*) giving through penetration and hence the maximum stress σ_f at the plain strain limit. Taking $a \approx 1.5\ t$ then

$$K = \sigma_f \sqrt{\pi a} = K_{Id} = 0.63\ \sigma_{yd} \sqrt{t} \quad \text{at } L$$

$$\therefore\ \sigma_f = \frac{0.63\ \sigma_{yd} \sqrt{t}}{\sqrt{\pi 1.5t}} = \frac{0.63\ \sigma_{yd}}{\sqrt{1.5\pi}} \approx 0.3\ \sigma_{yd}$$

In the later version of the diagram (6) the *L* point is set at 0.2 σ_{yd}. It should also be noted that in the Pellini diagram the crack arrest line is horizontal up to the *L* point which, for thick plate, could be well beyond the NDTT, whereas in the earlier Fracture Analysis Diagram, the curve started to rise immediately after the NDTT. This point will be further explored in a later section. Two other features of the Pellini approach are worth noting, particularly as they relate to Arctic grade steels.

The first is that the location of the *L* and *YC* points refer to dynamic toughness levels on a very flat part of the dynamic toughness-temperature curve. Thus their position with respect to the NDTT will be extremely sensitive to the precise rise of the toughness curve and to the level of dynamic toughness at the NDTT. Even small differences among materials in the toughness around NDTT could have a very substantial effect on the position of the *L* and *YC* points relative to the NDTT.

The second point is that for the purposes of establishing guidelines a constant value of dynamic yield strength is assumed. When the method, however, is applied to higher strength materials, and particularly to lower temperature applications, the dynamic yield

strength may be substantially higher than that assumed by Pellini. This is particularly so if the method is to be used for developing toughness requirements for Arctic structures. For example, for a room temperature static yield strength of 350 MPa and a temperature of –50°C, the dynamic yield strength is estimated to be 634 MPa (based on an equation developed in Appendix A). The higher dynamic yield strength has the effect of increasing the toughness at the *L*, *YC* and also NDTT points. Assuming that the toughness values for these points can still be read from the Pellini reference toughness curve, the diagram has been redrawn in Fig. 4 for the value $\sigma_{yd} = 634$ MPa. It is seen that the lines have shifted about 6°C to the left. This is because the reference toughness line curves up, and for higher values of σ_{yd}, the NDTT, *L*, and *YC* points become closer together. For even higher strength steels, such as those proposed for the Polar 8 Arctic icebreaker, (yield strength 440 MPa), the shift may be even more at -50°C.

Review of Crack Arrest Data

In order to compare the CSA S473 requirements and the NDTT approach directly with fracture performance of Arctic grade steels, results of crack arrest tests were collected. Data was obtained from published literature and steel company publications (7-19) and a database of over 250 entries was established. The data covered a range of test types, specimen thicknesses, and steel types and was considered a sufficiently large sample for the purposes of this study. One difficulty encountered was that most crack arrest data was reported in the form of graphs which inevitably introduced some error in extracting the values. In a few cases printing errors were noted in the published graphs. To minimize errors, graphs were enlarged several times before determining the coordinates of each datapoint.

Test Types

The majority of the results were from Japanese tests using the standard double tension test. This is a temperature gradient test and K_{ca} values are calculated on the basis of static fracture mechanics. A few tests were from Esso tests using larger plates. Approximately 55 points were from experiments using the Compact Crack Arrest (CCA) test developed by MRL and described in ASTM Standard E1221-88 (20). For comparative purposes approximately 50 results of dynamic initiation fracture toughness measured with instrumented Charpy or three point bend specimens on older ship grade steels were included. A few results from double cantilever beam specimens were also included.

Crack arrest data was only included where either CVN or NDTT information was provided. In many cases only one or the other was given and therefore analysis of results with respect to CVN and NDTT are from separate databases although there is considerable overlap. The complete database where NDTT information was available is listed in Table 2.

Analysis

Nakano and Tanaka (15) published crack arrest data covering a range of steel types, thicknesses, and test techniques. They showed very poor correlation between crack arrest toughness and the NDTT (Fig. 5) and concluded that a better correlation existed with the CVN test. The drop weight test, however, is not expected to measure a crack arrest toughness directly. As a number of authors have pointed out (18, 21) the NDTT should correspond to a constant value of K_{Id}/σ_{yd}. The value of σ_{yd} will be a function both of the room temperature yield strength of the material and the temperature. The surface of the drop weight specimen

suffers a strain exceeding 1% and therefore yields even when the yield stress is greatly elevated by dynamic loading rates or low temperatures. Values of σ_{yd} were therefore estimated for all results using two methods of estimation. One formula quoted by Tyson (18) is:

$$(\sigma_y)_{T,t} = \sigma_{RT} + \frac{666{,}500}{T_{(°K)} \log(2 \times 10^{10} \tau)} - 190 \qquad \text{.....1)}$$

where σ_{RT} is the 'static' room temperature yield strength, T is the absolute temperature and τ is the duration of the test. This formula includes the effect of strain rate and temperature but does not recognize the diminishing effect of these as the yield strength increases. A revised equation was therefore developed from data published by Shoemaker et al. (19) for steels up to ≈ 1000 MPa yield strength. The derivation is given in Appendix A and resulted in the equation:

$$(\sigma_y)_{T,\,\dot{\varepsilon}} = \sigma_{RT} + \frac{1850 - \sigma_{RT}}{\left[T_{(°K)} \ln\left\langle\frac{10^8}{\dot{\varepsilon}}\right\rangle\right] \times 10^{-3}} - 157$$

where $\dot{\varepsilon}$ is the strain rate. For dynamic crack arrest or drop weight tests the formula reduces to:

$$\sigma_{yd} = \sigma_{RT} + \frac{1850 - \sigma_{RT}}{16.1 \times 10^{-3} \times T_{(°K)}} - 157 \qquad \text{.....2)}$$

The overall results are not substantially affected by the choice of equation and most graphs developed in this report use the former.

When the Nakano and Tanaka data is replotted in the form K_{ca}/σ_{yd} against T - NDTT, excellent correlation results. This is best shown in Figs. 6 and 7 where a logarithmic scale is used for the vertical axis. The data covers yield strengths from 314 to 785 MPa and NDTT temperatures from -60 to -25°C. The data also suggests a good linear relation between log K_{ca}/σ_{yd} and T - NDTT over a wide temperature range.

Japanese crack arrest data is normally plotted in the form of log K_{ca} against $1/T_{(°K)}$. The slopes of such lines are reported (22) to vary with the material in the range -474 to -1252 and appear to depend on the temperature. This form of plot, however, creates difficulties when using temperature normalized with respect to the NDTT, and was not used.

In Fig. 8 all results except those from the old ship steels are plotted directly against normalized temperature. Considerable scatter is obvious, although a lower bound curve could readily be drawn. In Fig. 9 all results are plotted against the temperature normalized with respect to the Charpy V notch, 50% shear fracture appearance transition temperature, and even greater scatter is observed. This result confirms the view that the drop weight test is more reliable than the CVN test for indicating crack arrest behaviour. In Fig. 10 K_{ca} data is plotted in logarithmic form and in Fig. 11 K_{ca} is normalized with respect to the dynamic yield strength estimated from Equation 1. The correlation is greatly improved when account is taken of the dynamic yield strength.

Analysis of Scatter

Although the NDTT gives a better indicator of crack arrest behaviour than the CVN transition temperature, there is still considerable scatter in Fig. 11, and a toughness requirement based on a lower bound curve drawn around the data will lead to very conservative requirements for many steels. An attempt was therefore made to determine the sources of scatter.

Test results of individual steels usually comprise 4 or 5 data points at different temperatures for the same test type. When plotted in the form $\log K_{ca}/\sigma_{yd}$ against T - NDTT, good straight lines are always obtained. An example is shown in Fig. 12. Regression analysis was performed on all the groups in an attempt to identify effects of test technique, thickness, or steel type.

Effect of Thickness

Thicknesses ranged from 22 mm to 250 mm although the majority of test results were from plates in the range 32-40 mm. Data was grouped according to thickness and regression analysis performed. No effect of thickness could be detected, there being wide variations in the position of the crack arrest curve for each thickness range.

The data for 250 mm thick plate did lie at higher temperatures, but several results of thinner plates also showed low K_{ca} values at higher temperatures. Similarly, many results in all thicknesses up to 50 mm showed high values of K_{ca} even at the NDTT.

This does not mean that thickness has no effect but rather that other factors are more dominant. In general, data for each heat of steel is only available for a single thickness, and thus steel-to-steel or heat-to-heat variations in toughness cannot be separated from those due to thickness. Only in one report (17) was a plate machined to two thicknesses to measure

thickness effects directly. This showed the expected shift to higher temperatures for the thicker sections.

Effect of Test Type

Most of the double tension results were at temperatures above NDTT, and the slopes of the lines here were higher than those of the compact crack arrest tests which were usually carried out at temperatures below the NDTT. Table 3 shows the mean and standard deviation of the slopes and intercepts of the lines from the various tests. The range of slopes for the double tension tests was wider than the equivalent values reported by Smedley (22) although the mean slope was similar. The slope was even lower for the K_{Id} data from old ship steels which are shown in Fig. 13. Note that the linear relation between $\log K_{Ia}/\sigma_{yd}$ and T - NDTT is maintained over a very wide temperature range. Some of the slope, but not all, can be attributed to the increase in σ_{yd} with decreasing temperature.

It is of interest to compare the intercepts of these lines at T - NDTT = 0°C with the 'theoretical' values from analysis of the drop weight specimen. Theoretical analysis of the drop weight test has been discussed by several authors (18, 21) and is not repeated here. The analysis suggests that the dynamic toughness at the NDTT should be given by:

$$K_{ID}/\sigma_{yd} \approx 0.075 \quad (\text{MPa}\sqrt{\text{m}},\ \text{MPa})$$

The intercept from the K_{Id} data gives a value 0.073, in close agreement with that expected. The double tension tests give a value of 0.071 based on the mean intercept but the considerable scatter should be noted. The CCA test data with comparatively little scatter gave a value of 0.155 for K_{Ia}/σ_{yd}, over twice the expected figure.

The good linear relation was maintained by all tests regardless of temperature. Thus CCA tests on very thick sections at temperatures well above the NDTT still fitted the CCA line for lower temperatures. It is assumed that only CCA results that were reasonably 'valid' (i.e., close to plain strain conditions) were reported. Similarly, the steeper slope of the double tension K_{ca} data was still maintained for data points well below the NDTT.

A noticeable feature of the double tension results is that many values of K_{ca} around the NDTT fell well below the K_{Ia} or K_{Id} values from other tests. This is illustrated in Fig. 14 taken from reference (10) where several different types of tests were conducted on the same steel.

A discussion of the significance of the toughness value measured by the various tests

is beyond the scope of this report, but the conclusion of the present analysis is that test method has a major effect on the crack arrest toughness measured as it relates to the NDTT. The NDTT appears to predict K_{Id} well, and there is a good correlation with K_{Ia} from CCA tests, although K_{Ia} around the NDTT is higher than K_{Id}. It should be noted in Fig. 11 that many of the K_{ca} values from double tension tests lie below the Pellini (K_{Id}) reference toughness curve and a few below the ASME curve. There is no reason, a priori, to expect agreement between the K_{ca} values and the reference toughness curve based on K_{Id} measurements. K_{ca} values are calculated from double tension tests using static linear elastic fracture mechanics, although crack arrest in these tests is under elastic-plastic conditions. Most of the double tension test data is from temperature gradient tests which pose some difficulties in establishing the crack length and exact point of arrest.

The greatest scatter in the present results was within the double tension tests, and an attempt was made to find a reason for this. Data which fell on or below the Pellini curve and those that fell well above were further analyzed. The relevant data is summarized in Tables 4 and 5.

The first possibility for low K_{ca} values was that the NDTT was abnormally low. A low NDTT could arise from higher than average toughness on the plate surface where the drop weight test crack starter bead is deposited, or it could arise from the formation of a tough HAZ around the crack starter. It is also possible that the P3 drop weight specimen could be too thin to measure the NDTT correctly in some steels. (The specimen size is not usually reported in the literature). In all cases this should result in a low NDTT relative to other toughness tests such as the CVN. Examination of Table 4, however, shows that many of the tests with low K_{ca} also had CVN transition temperatures well below the NDTT. Thus an abnormally low NDTT is not sufficient to explain the K_{ca} results.

Study of the data in Table 4 failed to reveal any effect of steel type, thickness, yield strength, composition, or other feature that could explain the results. On the other hand, there are reasons to explain why the crack arrest toughness relative to the NDTT may be significantly improved. Japanese authors (8) have drawn attention to the effect of 'splitting' on improving crack arrest toughness. Splitting occurs in a certain temperature range when the through-thickness stresses cause cleavage fractures parallel to the plane of the main crack. It is most effective when there is an optimum difference in toughness between the through-thickness direction and the direction (longitudinal or transverse) of the main crack. It is very apparent in TMCP steels. Fig. 15, taken from Reference 8, shows the effect of splitting index on the crack arrest properties in general terms, but splitting index could not be tied to individual crack arrest results in the present work.

Analysis of CSA S473 Requirements

The basis of the crack arrest requirements of Clause 6 of CSA S473 are contained in the commentary to the Standard. The drop weight test temperatures for moderate and good crack arrest are determined from the Pellini diagram. Good crack arrest corresponds to arrest of cracks under a nominal stress of $0.6F_y$ (F_y is the specified minimum yield strength) and moderate crack arrest under a stress of $0.2F_y$. The latter criterion corresponds to the *L* point on the Pellini diagram. The corresponding temperatures are shown for the various thicknesses in Fig. 16. Assuming that the NDTT is 5°C below the no-break temperature, the drop weight test temperatures for no-break performance are established and are summarized in Table 6. As pointed out earlier, the test temperatures would be about 6°C higher if the Pellini diagram is modified to take account of the higher dynamic yield stress for 350 MPa grade steel and -50°C temperatures.

Moderate Crack Arrest Capability

The criterion for moderate crack arrest capability was selected on the Pellini diagram at $0.2F_y$. Qualitatively, crack arrest of a large crack at $0.2F_y$ may correspond to arrest of a smaller crack at a higher stress, and in that sense represents moderate crack arrest capability. Since the $0.2F_y$ criterion corresponds to the *L* point, conditions of plane strain are maintained up to this temperature. The crack arrest capability may therefore be estimated quantitatively from the Pellini reference toughness curve using fracture mechanics . This curve rises above the NDTT, and therefore under plane strain conditions the crack tolerance increases with increasing temperature above the NDTT. This is not reflected in the Pellini diagram because the *L* positions are marked on a horizontal line at $0.2F_y$. For thick sections, however, where the limit of plane strain capacity may be well above the NDTT, the dynamic fracture toughness can be quite high and the plane strain crack tolerance large.

Based on the Pellini reference curve(6) and a nominal stress of 210 MPa (0.6 x 350), the crack tolerance (i.e., critical crack size for a through-thickness crack) relative to NDTT has been drawn in Fig. 17. Based on this curve, the crack tolerance for moderate(at $0.2F_y$) and good (at $0.6F_y$) crack arrest corresponding to the CSA S473 requirements have been calculated and are shown in Table 7. It is noted that the plane strain crack tolerance for moderate crack arrest increases markedly with increasing thickness because the *L* point has been selected as the criterion. Thus thicker steel meeting CSA S473 moderate arrest requirements would have significantly better crack arrest capability than thinner steel. Since

the moderate crack arrest criterion corresponds to plane strain conditions, it is difficult to justify an increase in crack tolerance with increasing thickness, and the moderate crack arrest requirement may be unduly conservative.

If moderate crack arrest is based on a fixed crack tolerance under plane strain conditions, then this would be independent of thickness. For example, at NDTT + 5 (i.e., no-break at the minimum design temperature) crack tolerance is $a = 6$ mm for an equivalent through-crack at the yield stress. This criterion would be adequate to prevent dynamic initiation or pop-in from small flaws around the weld but would not arrest a large propagating crack that had run out of the weld zone if stresses were high. Such a criterion might be considered adequate for redundant members where only local damage could arise from a fracture. A drop weight test at around the NDTT also has direct structural significance and does not rely on any assumed correlation between drop weight behaviour and large crack arrest fracture behaviour. Such a criterion is also easily understood by the designer both in terms of what the steel is capable of doing and, more importantly, what the steel is not capable of doing.

It is worth exploring the resistance to crack initiation under intermediate strain rates at the NDTT. If a strain rate of 10^{-3} secs^{-1} is assumed for intermediate loading, then the temperature shift between dynamic and intermediate rates using Barsom's data (23) is about 55°C. This loading rate is faster than recorded in offshore structures such as the SSDC (24) but may be slower than recorded in icebreakers. Based on the Pellini reference toughness curve, the value of K_{Id} under fast loading 55°C above the NDTT is 144 MPa$\sqrt{m}$. Therefore, under intermediate loading rates K_{Ic} at the NDTT is estimated to be 144 MPa$\sqrt{m}$. Using this value, the minimum thickness to maintain plane strain conditions is 439 mm and the minimum thickness for through thickness yielding is 174 mm. For a through-crack under plane strain conditions at a stress 0.6 Fy, the critical size is:

$$a = \frac{1}{\pi}\left(\frac{K_{Ic}}{\sigma}\right)^2 = \frac{1}{\pi}\left(\frac{144}{210}\right)^2 \approx 150 \text{ mm}$$

It is concluded from this analysis that a steel meeting a moderate crack arrest criterion of no-break at the minimum service temperature would have a very high initiation toughness under intermediate loading rates with excellent crack tolerance up to very thick sections. Such a criterion exceeds AASHTO criteria for highway bridges (23) and would allow large fatigue cracks to be accommodated without initiating brittle fractures.

This alternative moderate arrest criterion should also be applicable to box 3 of the Standard even though this applies to non-redundant members. In box 3, members are only

subject to compressive stresses , and the justification for toughness requirements rests with the possibility of residual tension stresses. Large scale tension residual stresses extending throughout the member are unlikely in a non-redundant case, and if they were recognized the designer would be prudent to elevate the member to box 6 or 9.

Good Crack Arrest

The 'good' crack arrest criterion is intended to represent full crack arrest i.e., the point at which crack arrest occurs under elastic-plastic conditions regardless of crack length. The 'good' crack arrest criterion is, of course, arbitrary and does not guarantee crack arrest under all circumstances. The arrest of a large running crack is a complex phenomenon depending on, among other things, the behaviour of the structure itself. Bulging, instability, reflected stress waves, and other forces come into play in the arrest behaviour of long cracks. The experimental evidence shows that large cracks running under high stresses arrest when entering tougher material under elastic-plastic conditions. Arrest is preceeded by tunneling in which the crack front at the centre of the plate runs ahead of that at the edge where the plastic zone is larger. A crack needs to run about 3X plate thickness for tunneling to be established.

The crack arrest criterion based on the Pellini approach attempts to define the elastic-plastic stress state transition by estimating plastic zone size from the dynamic plane strain fracture toughness. It is not based on a fracture mechanics determination of crack tolerance. As the plate thickness increases, so the elastic-plastic stress state transition moves to higher temperatures. For these conditions, the plane strain fracture toughness is also increasing, and thus the plane strain crack tolerance also increases. The rise in plane strain toughness is only recognized in the Pellini diagram in so far as it affects the location of the *L* and *YC* points. But it is not included in determining crack tolerance for crack arrest. It is thus possible at temperatures above the NDTT for the critical crack size for dynamic initiation or continued propagation to be larger than the actual crack size, and a plane strain arrest could occur. This is indeed the situation artificially created in the compact crack arrest test.

It is of interest to calculate the (plane strain) crack tolerance corresponding to the good crack arrest criterion. These are shown in Table 7. The critical values of a are roughly equal to the plate thickness.

A more useful comparison is made between the good crack arrest criterion and the results of crack arrest tests reviewed earlier. It was noted that many of the K_{ca} values reported for double tension tests fell below the K_{Id} values inherent in the Pellini toughness curve. For thin sections in which crack arrest occurs under elastic-plastic conditions, no direct

comparison can be made between the K_{ca} values and the Pellini crack arrest criterion. However, in so far as the K_{ca} values are determined from tests on large plates, a value of K_{ca} corresponding to arrest of a large crack at 0.6 Fy can be determined and the crack arrest temperature compared with the Pellini criterion. To do this the K_{ca} data has been statistically analyzed in the following way. It is assumed that a lower bound design line can be represented by the equation:

$$\log\left(\frac{K_{ca}}{\sigma_{yd}} \times 10^3\right) = A\,(T - \text{NDTT}) + B$$

The value of $A = 0.0115$ is determined by drawing the lower bound line through the data. This is simply a line above which all the data above T - NDTT = –20°C lie. From all data, the mean and standard deviation of B is then determined giving $B = 1.98$ (mean) and standard deviation = 0.203. Assuming the data can be represented by a normal distribution, the value of B is determined that gives a design line for which there is a 95% probability that the toughness will exceed it. This then gives the following equation which also corresponds to the 5% percentile of the data sample.:

$$\log\left(\frac{K_{ca}}{\sigma_{yd}} \times 10^3\right) = 0.0115\,(T - \text{NDTT}) + 1.646 \qquad \text{.....3)}$$

To establish a 'good' crack arrest criterion in terms of crack size it is worth considering the conditions under which arrest might occur in practice. In one case, a fast crack running across a plate under the applied stress might arrest on entering the tougher adjacent plate. Such a criterion has been applied to crack arrest design of storage tanks. Another situation might be where a brittle crack initiates in a weld and first propagates under the influence of residual stresses. Arrest occurs on running out of the weld and residual stress tension zone into the plate. This may involve a drop in stress and a change of toughness. If arrest does not occur at this point, the crack may not get a second chance to arrest until it has run across the entire plate.

The width of the residual tension zone depends on the heat input of individual weld passes. Masubuchi (25) shows values for the tension zone half-width of 50-75 mm for plates 13-16 mm thick. For multipass welds in thick plates the residual stress distribution is complex, but a maximum value of 100 mm is not unreasonable for typical welds. Very high heat input single pass welds, however, could have tension zones substantially exceeding this. For the purposes of establishing a crack arrest criterion by equating a critical crack size to the width of the tension zone, a figure of $a = 100$ mm is not unreasonable. This value has also been adopted by WES 3003 for a crack arrest criterion.

A value of a = 100 mm and a stress of 210 MPa (0.6 Fy) leads to a value of K_{ca} = 118 MPa$\sqrt{m}$. Using a value σ_{yd} = 625 MPa for 350 grade material at -45°C gives a value of log K_{ca}/σ_{yd} x 10^3 = 2.276. Inserting this into Equation 3 which is based on all the data, a value of T - NDTT = 55°C is obtained.

This analysis was repeated with the data divided into three groups of thickness range and gave the results:

t = 50 - 250 mm, T - NDTT = 53°C
t = 30 - 40 mm, T - NDTT = 56°C
t = 20 - 25 mm, T - NDTT = 38°C

The calculation was repeated for other crack sizes and the results of the analysis are shown in Table 8. The results show that the temperature shifts T - NDTT are greater than the CSA S473 requirements even for relatively small cracks of 50 mm. To determine the crack tolerance for steels meeting CSA S473 criteria, Equation 3 was used to calculate K_{ca} for values of T - NDTT corresponding to CSA S473 requirements. Results are shown in Table 9. For a steel meeting the CSA S473 criteria there is a 95% probability that the crack tolerance is better than that given in Table 9.

General Discussion and Conclusions

The present work has shown that the NDTT measured by the drop weight test correlates well with crack arrest and dynamic toughness measured by a compact crack arrest and dynamic initiation tests when account is taken of the effects of yield strength and temperature on the dynamic yield stress. There is, however, considerable scatter in the relation between K_{ca} measured by temperature gradient tests such as the double tension and Esso tests and the NDTT. This scatter could not be attributed to abnormally low NDTT's or to any particular aspect of the steel, although TMCP steels prone to splitting are known to have exceptionally good crack arrest properties. Based on the data reviewed in the present work, the CSA S473 requirements corresponding to good crack arrest would have ensured arrest of cracks in the majority of cases, but for a few steels short cracks would not have been arrested. For most cases, the CSA requirements appear to be conservative. If the CSA requirements were based on the lower bound of all the K_{ca} data reviewed here, such a requirement would be overly conservative for the majority of cases.

The good crack arrest criterion is, of course, arbitrary and there is a strong incentive when dealing with fracture critical members (boxes 6 and 9) to examine each case on its own merits. For cases where the applied stress away from the weld is low, the current CSA S473 requirements may be adequate to ensure good crack arrest. For fracture critical members under high stress, there is clearly a strong incentive to develop crack arrest data on the intended steel and correlate this back to drop weight or CVN properties for quality control purposes. The wide scatter, however, in K_{ca} values and the lack of any obvious feature of the steel to explain the relation with NDTT implies that experimentally measured values of K_{ca} are strictly applicable only to the plate tested. Extrapolation to other thicknesses or heats of the same steel should be done with the utmost caution, although the Japanese work on splitting index suggests that at least some of the characteristics that promote good crack arrest toughness can be defined.

Although the analysis based on double tension tests indicates that under some circumstances the CSA S473 requirement may be unconservative, the wide scatter of results suggests that a revision of CSA S473 is not warranted. A revision of the commentary, however, that would advise the designer on the shortcomings of the good crack arrest requirements is advisable. It is also recommended that the wording of the Standard be modified to encourage crack arrest testing of steels of fracture critical members that could result in a more economic selection of steel. In this context, the significance of the double

tension temperature gradient test needs exploring, and alternate tests may be considered more structurally representative.

In the present version of CSA S473, there is little difference in the requirements between good and moderate crack arrest. This is because the *L* point was selected as the moderate crack arrest criterion. The analysis shows that an alternate moderate crack arrest criterion of no-break in the drop weight test at the minimum toughness design temperature provides a bigger spread between the two criteria and would thus provide a more useful option to the designer. Such a criterion provides some protection from brittle pop-in, the traditional cause of brittle fracture, as well as providing excellent resistance to fracture initiation under intermediate loading rates.

References

Note: The second number is the author's file number and is the number appearing in the database in Table 2.

1) 84-11 Marshall, P.W. "Welding of Tubular Structures," Houdremont Lecture, IIW, Boston, 1984.

2) 75-13 "Conducting Drop-Weight Test to Determine Nil-Ductility Transition Temperature of Ferritic Steels," ASTM E208.

3) 88-17 Graville, B.A. "Correlations between Charpy Properties and the Nil-Ductility Transition Temperature," Project I-1 CSA Verification Program for Offshore Structures Code. CSA 1988.

4) 71-4 Pellini, W.S. "Principles of Fracture-Safe Design." *Welding Journal Research Supplement* (Part 1) March, pp. 91-s to 109-s and (Part 2) April, pp. 147-s to 162-s, 1971.

5) 73-12 Pellini, W.S. "Analytical Design Procedures for Metals of Elastic-Plastic and Plastic Fracture Properties." In *Proceedings of Joint U.S.-Japanese Symposium on Application of Pressure Components Codes*, Tokyo, March 13-15, 1973.

6) 83-19 Pellini. W.S. "Guidelines for Fracture-Safe and Fatigue-Reliable Design of Steel Structures." The Welding Institute, 1983.

7) 88-13 Ono, Y., Uchino, K., Matsuda, S., Satoh, T., Okamura, Y., Yamamoto, K., Ikeda, K. "Development of Low Temperature Steel for Welding with High Heat Input." *Nippon Steel Technical Report*, No. 36, Jan. 1988, pp. 49-59.

8) 88-11 Japan Pressure Vessel Research Council, "Review of Properties of TMCP Steel-Pressure Vessel Steels for Low Temperature Service." *Welding Research Council Bulletin*, No. 334, June, 1988.

9) 86-43 Watanabe, I. "Thermo-Mechanically Controlled Rolled Steels and Their Properties." *International Symposium on Fracture-Safe Designs for Large Storage Tanks.* The Welding Institute, 1986, pp. 195-204.

10) 86-44 Kawaguchi, Y., and Willoughby, A.A. "Crack Arrest Tests and their Use for Evaluating Material Properties." *International Symposium on Fracture-Safe Designs for Large Storage Tanks.* The Welding Institute, 1986, pp. 179-192.

11) 86-46 Bristoll, P., and de Koning, A.C. "Crack Arrest Capability of a Controlled Rolled Q&T 3 1/2 Nickel Steel." *International Symposium on Fracture-Safe Designs for Large Storage Tanks.* The Welding Institute, 1986, pp. 151-167.

12) 86-20 Nakano, N., Bessyo, K., Iida, Y., Seta, I., Kamada, Y. "Developments in Materials for Arctic Offshore Structures." *Offshore Mechanics and Arctic Engineering (OMAE)* Conference, Tokyo, April, 1986. Publ. ASME.

13) 83-18 Kawasaki Steel Corporation, Technical Reports (MACS). 1983. (Company Reports on MACS Steel).

14) 83-15 Kozasu, I. "Metallurgical Design and Properties of Structural Steel for Arctic Use." *Proceedings of a Study Session on Fracture Evaluation of Steels for Arctic Marine Use*, Oct. 1983, Ottawa, ed. Thomson,R., and Champion, C.S. (CANMET).

15) 82-40 Nakano, Y., and Tanaka, M. "Crack Arrest Toughness of Structural Steels Evaluated by Compact Test." *Trans. Iron and Steel Institute of Japan*, Vol. 22, 1982, pp 147-153.

16) 86-30 Nozaki, N., Bessyo, K., Ozawa, H., Kawaguchi, Y. "Fracture-Safe Steel Plate for LPG Tanks 2.5% Ni SHT." *Sumitomo Search*, No. 32, May, 1986, pp. 53-62.

17) 82-7 Ripling, E.J., and Crosley, P.B. "Crack Arrest Fracture Toughness of a Structural Steel (A36)." *Welding Journal*, Vol. 63 No. 3, Research Supplement, pp. 65-s to 74-s, March, 1974.

18) 84-13 Tyson, W., and Harbec, J. "Dynamic Toughness: Fracture Mechanics Interpretation of the Drop-Weight (NDT) Test." *International Journal of Fracture*, 25, 1984, pp. 133-141.

19) 71-3 Shoemaker, A.K., and Rolfe, S.T. "The Static and Dynamic Low Temperature Crack Toughness Performance of Seven Structural Steels." *Engineering Fracture Mechanics*, Vol. 2, pp. 319-339, 1971.

20) 88-16 "Standard Method for Determining Plane Strain Crack Arrest Fracture Toughness K_{Ia} of Ferritic Steels," ASTM Standard E1221-88.

21) 67-4 Irwin, G.R., Krafft, J.M., Paris, P.C., Wells, A.A. "Basic Aspects of Crack

Growth and Fracture," NRL report 6598. Washington, D.C., Nov. 21, 1967, (82p).

22) 86- Smedley, G.P., and Viner, A.C. "Selection of Steels for Hull Structures of Ships." *International Symposium on Fracture-Safe Designs for Large Storage Tanks.* The Welding Institute, 1986, pp. 69-82.

23) 75-10 Barsom, J.M. "The Development of the AASHTO Fracture Toughness Requirements for Bridges." AISI, Wash. DC., Feb. 1975, (63p).

24) 83- Ghoneim, G.A.M., and Johansson, B.M. "Fracture Toughness Requirements for Arctic Steels in Static and Dynamic Applications." *Proceedings of a Study Session on Fracture Evaluation of Steels for Arctic Marine Use*, Oct. 1983, Ottawa, ed. Thomson, R., and Champion, C.S. (CANMET).

25) 80- Masubuchi, K. "Analysis of Welded Structures." Pergamon, 1980.

Table 1. Summary of CSA S473 drop weight test requirements

Test temperature (°C) for no-break performance.

Thickness (mm)	Box 1	Box 2	Box 3
$t \leq 26$	none	none	T
$26 < t \leq 38$			T – 10
$38 < t \leq 52$			T – 20
$52 < t$			T – 35
	Box 4	Box 5	Box 6
$t \leq 26$	none	T	T – 10
$26 < t \leq 38$		T – 10	T – 20
$38 < t \leq 52$		T – 20	T – 30
$52 < t$		T – 35	TBE*
	Box 7	Box 8	Box 9
$t \leq 26$	T	T	T – 10
$26 < t \leq 38$	T	T – 10	T – 20
$38 < t \leq 52$	T	T – 20	T – 30
$52 < t$	T – 20	T – 35	TBE*

*TBE = to be established
T is the toughness design temperature

Table 2. Complete Database of Crack Arrest Toughness with NDTT.

	A	B	C	D	E	F	G	H	I	J	K	L	M	N
1	Reference	File number	steel type	thickness mm	test type	Yield MPa	vTrs °C	NDT °C	T°C	Kca,Kid,Kia (MPa√m)	Dyn.yield at T	K/y XE3	T-NDT	Log K/Y
2	# 7	88-13	TMCP AcC	40	Esso TG	399	-90	-70	-40	234	662.978541	352.953	30	2.54772
3						399	-90	-70	-38	186	659.114894	282.197	32	2.45055
4						399	-90	-70	-50	155	683.336323	226.828	20	2.3557
5						399	-90	-70	-58	109	700.986047	155.495	12	2.19172
6						399	-90	-70	-91	45	790.192308	56.9482	-21	1.75548
7	# 8	88-11	TMCP A	32	DT & Esso TG	497	-132	-100	-77	155	846.678571	183.068	23	2.26261
8						497	-132	-100	-110	62	955.93865	64.8577	-10	1.81196
9			F			451	-160	-145	-77	264	800.678571	329.72	68	2.51815
10						451	-160	-145	-110	111	909.93865	121.986	35	2.08631
11						451	-160	-145	-123	84	966.18	86.9403	22	1.93922
12	# 9	86-43	Norm	35	DT TG	338	-79	-50	-5	232	542.690299	427.5	45	2.63094
13						338	-79	-50	-20	140	566.090909	247.31	30	2.39324
14						338	-79	-50	-35	49	592.441176	82.7086	15	1.91755
15						338	-79	-50	-50	26	622.336323	41.7781	0	1.62095
16			QT	32	DT TG	368	-86	-70	-15	285	587.988372	484.703	55	2.68548
17						368	-86	-70	-55	85	663.215596	128.163	15	2.10776
18						368	-86	-70	-60	55	674.605634	81.5291	10	1.91131
19						368	-86	-70	-68	39	693.985366	56.1972	2	1.74971
20			QR	40	DT TG	363	-92	-85	-38	178	623.114894	285.662	47	2.45585
21						363	-92	-85	-65	88	681.543269	129.119	20	2.11099
22						363	-92	-85	-68	60	688.985366	87.0846	17	1.93994
23			QLAC	40	DT TG	426	-128	-70	-23	278	659.108	421.782	47	2.62509
24						426	-128	-70	-30	208	671.296296	309.848	40	2.49115
25						426	-128	-70	-45	112	699.934211	160.015	25	2.20416
26						426	-128	-70	-62	81	737.312796	109.858	8	2.04083
27						426	-128	-70	-75	43	770.227273	55.8277	-5	1.74685
28			QLAC	32	DT TG	362	-103	-90	-29	261	605.512295	431.04	61	2.63452
29						362	-103	-90	-37	188	620.207627	303.124	53	2.48162
30						362	-103	-90	-47	142	640.039823	221.861	43	2.34608
31						362	-103	-90	-56	96	659.451613	145.576	34	2.16309
32						362	-103	-90	-66	46	683	67.3499	24	1.82834
33			CR 0.6Ni	32	DT TG	447	-112	-95	-53	246	737.804545	333.422	42	2.52299
34						447	-112	-95	-70	148	778.068966	190.215	25	2.27924
35						447	-112	-95	-73	95	785.885	120.883	22	2.08236
36						447	-112	-95	-167	20	1254.89623	15.9376	-72	1.20242
37			QLAC 1.5 Ni	40	DT TG	413	-166	-135	-98	215	827.44	259.838	37	2.4147
38						413	-166	-135	-100	108	834.427746	129.43	35	2.11204
39						413	-166	-135	-132	73	973.191489	75.0109	3	1.87512
40						413	-166	-135	-144	45	1042.97674	43.1457	-9	1.63494
41						413	-166	-135	-168	20	1230.4	16.2549	-33	1.21098
42			QLAC 2.5 Ni	40	DT TG	445	-165	-145	-95	151	849.252809	177.803	50	2.24994
43						445	-165	-145	-102	214	873.578947	244.969	43	2.38911
44						445	-165	-145	-108	111	896.072727	123.874	37	2.09298
45						445	-165	-145	-127	54	979.5	55.1302	18	1.74139
46						445	-165	-145	-128	76	984.496552	77.1968	17	1.8876
47	# 10	86-44	SHT2N37	34	CCT	452	-104	-110	-70	220	783.068966	280.946	40	2.44862
48						452	-104	-110	-78	247	804.446154	307.044	32	2.4872
49						452	-104	-110	-80	190	810.067358	234.548	30	2.37023
50						452	-104	-110	-90	136	840.016393	161.902	20	2.20925
51						452	-104	-110	-100	119	873.427746	136.245	10	2.13432
52						452	-104	-110	-106	136	895.39521	151.888	4	2.18152
53						452	-104	-110	-120	108	953.352941	113.284	-10	2.05417
54						452	-104	-110	-150	31	1121.97561	27.6298	-40	1.44138
55			"	"	TDCB	452	-104	-110	-90	167	840.016393	198.806	20	2.29843
56						452	-104	-110	-90	180	840.016393	214.282	20	2.33098

Table 2 continued.

	A	B	C	D	E	F	G	H	I	J	K	L	M	N
57						452	-104	-110	-100	140	873.427746	160.288	10	2.2049
58						452	-104	-110	-115	84	931.474684	90.1796	-5	1.95511
59						452	-104	-110	-115	100	931.474684	107.357	-5	2.03083
60						452	-104	-110	-130	56	1001.6993	55.905	-20	1.74745
61						452	-104	-110	-145	36	1088.38281	33.0766	-35	1.51952
62					DT TG	452	-104	-110	-87	207	830.693548	249.189	23	2.39653
63						452	-104	-110	-93	130	849.65	153.004	17	2.1847
64						452	-104	-110	-105	70	891.625	78.5083	5	1.89492
65	#11	86-46	CR/QT	22	DT TG	440		-125	-91	120	831.192308	144.371	34	2.15948
66						440		-125	-81	234	800.921875	292.163	44	2.46563
67						440		-125	-79	194	795.242268	243.951	46	2.3873
68						440		-125	-82	243	803.806283	302.312	43	2.48045
69						440		-125	-70	240	771.068966	311.256	55	2.49312
70	#12	86-20	A1 (DAC)	30	DT TG	417	-101	-90	-51	209	703.472973	297.097	39	2.4729
71						417	-101	-90	-73	131	755.885	173.307	17	2.23882
72						417	-101	-90	-91	82	808.192308	101.461	-1	2.0063
73						417	-101	-90	-106	51	860.39521	59.2751	-16	1.77287
74			A4	75	DT TG	377	-105	-90	-51	209	663.472973	315.009	39	2.49832
75						377	-105	-90	-65	100	695.543269	143.773	25	2.15768
76						377	-105	-90	-73	65	715.885	90.7967	17	1.95807
77						377	-105	-90	-83	33	743.721053	44.3715	7	1.6471
78	#13	83-18	C1 MACS	35	Esso	392	-90	-55	-29	260	635.512295	409.119	26	2.61185
79						392	-90	-55	-37	219	650.207627	336.815	18	2.52739
80						392	-90	-55	-55	123	687.215596	178.983	0	2.25281
81						392	-90	-55	-62	106	703.312796	150.715	-7	2.17816
82			C2	38	Esso	363	-125	-50	-50	169	647.336323	261.07	0	2.41676
83						363	-125	-50	-56	105	660.451613	158.982	-6	2.20135
84						363	-125	-50	-55	133	658.215596	202.061	-5	2.30548
85						363	-125	-50	-94	45	763.932961	58.9057	-44	1.77016
86	#14	83-15	A	25	DT TG	394	-96	-70	-42	320	661.909091	483.45	28	2.68435
87						394	-96	-70	-46	195	669.977974	291.054	24	2.46397
88						394	-96	-70	-68	170	719.985366	236.116	2	2.37313
89						394	-96	-70	-81	73	754.921875	96.6987	-11	1.98542
90						394	-96	-70	-111	30	856.944444	35.0081	-41	1.54417
91			C	38	DT TG	382	-94	-50	-10	295	594.193916	496.471	40	2.69589
92						382	-94	-50	-20	220	610.090909	360.602	30	2.55703
93						382	-94	-50	-45	95	655.934211	144.832	5	2.16086
94						382	-94	-50	-55	43	677.215596	63.4953	-5	1.80274
95			E	32	DT TG	392	-145	-105	-50	260	676.336323	384.424	55	2.58481
96						392	-145	-105	-52	320	680.628959	470.153	53	2.67224
97						392	-145	-105	-58	200	693.986047	288.19	47	2.45938
98						392	-145	-105	-72	145	728.253731	199.106	33	2.29909
99						392	-145	-105	-112	75	859	87.3108	-7	1.94107
100			F	32	DT TG	401	-139	-110	-52	280	689.628959	406.015	58	2.60854
101						401	-139	-110	-70	95	732.068966	129.769	40	2.11317
102						401	-139	-110	-80	160	759.067358	210.785	30	2.32384
103						401	-139	-110	-99	42	818.913793	51.2874	11	1.71001
104			G	34	DT TG	388	-130	-120	-26	310	626.246964	495.012	94	2.69462
105						388	-130	-120	-47	220	666.039823	330.311	73	2.51892
106						388	-130	-120	-69	145	716.514706	202.368	51	2.30614
107						388	-130	-120	-96	85	795.610169	106.836	24	2.02872
108						388	-130	-120	-130	50	937.699301	53.322	-10	1.72691
109			H	40	DT TG	422	-122	-70	-25	260	658.520161	394.825	45	2.5964
110						422	-122	-70	-31	205	669.095041	306.384	39	2.48627
111						422	-122	-70	-62	80	733.312796	109.094	8	2.0378
112						422	-122	-70	-75	41	766.227273	53.5089	-5	1.72843

Table 2 continued.

	A	B	C	D	E	F	G	H	I	J	K	L	M	N
113	#15	82-40	KD32	30	CCA	314	-14	-35	-100	46.5	735.427746	63.2285	-65	1.80091
114						314	-14	-35	-60	58.9	620.605634	94.9073	-25	1.9773
115						314	-14	-35	-40	72.8	577.978541	125.956	-5	2.10022
116						314	-14	-35	-20	99.2	542.090909	182.995	15	2.26244
117					Esso	314	-14	-35	-7	118	521.657895	226.202	28	2.3545
118						314	-14	-35	-1	153	512.886029	298.312	34	2.47467
119						314	-14	-35	-1	181	512.886029	352.905	34	2.54766
120						314	-14	-35	5	188	504.492806	372.651	40	2.5713
121						314	-14	-35	15	453	491.28125	922.079	50	2.96477
122					DC8	314	-14	-35	-50	37.2	598.336323	62.1724	-15	1.7936
123						314	-14	-35	-40	51.2	577.978541	88.5846	-5	1.94736
124						314	-14	-35	-30	107	559.296296	191.312	5	2.28174
125						314	-14	-35	-10	140	526.193916	266.062	25	2.42498
126			A533BCl.1.	250	CCA	488	-3	-25	-100	32.5	909.427746	35.7368	-75	1.55312
127						488	-3	-25	-100	43.4	909.427746	47.7223	-75	1.67872
128						488	-3	-25	-100	60.5	909.427746	66.5254	-75	1.82299
129						488	-3	-25	-75	46.5	832.227273	55.8742	-50	1.74721
130						488	-3	-25	-75	55.8	832.227273	67.049	-50	1.82639
131						488	-3	-25	-75	71.3	832.227273	85.6737	-50	1.93285
132						488	-3	-25	-50	112	772.336323	145.015	-25	2.16141
133						488	-3	-25	-25	96	724.520161	132.501	0	2.12222
134						488	-3	-25	-25	112	724.520161	154.585	0	2.18917
135						488	-3	-25	-25	138	724.520161	190.471	0	2.27983
136						488	-3	-25	0	124	685.461538	180.9	25	2.25744
137						488	-3	-25	10	125	671.770318	186.076	35	2.26969
138						488	-3	-25	10	153	671.770318	227.756	35	2.35747
139						488	-3	-25	10	166	671.770318	247.108	35	2.39289
140					Esso	488	-3	-25	-117	29.5	976.057692	30.2236	-92	1.48035
141						488	-3	-25	36	155	640.320388	242.066	61	2.38393
142						488	-3	-25	52	236	623.467692	378.528	77	2.5781
143						488	-3	-25	56	262	619.510638	422.914	81	2.62625
144			HT80-1	25	CCA	771	-110	-60	-100	94.6	1192.42775	79.3339	-40	1.89946
145						771	-110	-60	-80	150	1129.06736	132.853	-20	2.12337
146						771	-110	-60	-70	187	1102.06897	169.681	-10	2.22963
147						771	-110	-60	-60	271	1077.60563	251.483	0	2.40051
148			HT80-2	50	CCA	785	-78	-25	-95	80.6	1189.25281	67.7736	-70	1.83106
149						785	-78	-25	-75	88	1129.22727	80.2182	-50	1.77973
150						785	-78	-25	-55	76	1080.2156	70.3563	-30	1.8473
151						785	-78	-25	-45	124	1058.93421	117.099	-20	2.06855
152						785	-78	-25	-38	88	1045.11489	65.0646	-13	1.81334
153						785	-78	-25	-15	153	1004.98837	152.241	10	2.18253
154	#16	86-30	2.5 Ni	34	DTTG	470	<-120	-130	-94	285	870.932961	327.235	36	2.51486
155						470	<-120	-130	-99	190	887.913793	213.985	31	2.33038
156						470	<-120	-130	-108	187	921.072727	203.024	22	2.30755
157	#17	82-7	A36	51	CCA	270		-8	51	168	406.472222	413.312	59	2.61628
158						270		-8	40	130	417.945687	311.045	48	2.49282
159						270		-8	20	100	441.013652	226.75	28	2.35555
160						270		-8	20	101	441.013652	229.018	28	2.35987
161						270		-8	20	108	441.013652	244.89	28	2.38897
162						270		-8	-25	74	506.520161	146.095	-17	2.16463
163						270		-8	-25	65	506.520161	128.327	-17	2.10832
164						270		-8	-25	66	506.520161	130.301	-17	2.11495
165						270		-8	-50	60	554.336323	108.238	-42	2.03438
166						270		-8	-50	56	554.336323	101.022	-42	2.00441
167						270		-8	-50	52	554.336323	93.8059	-42	1.97223
168				25	CCA	283		-6	10	116	466.770318	248.516	16	2.39535

Table 2 continued.

	A	B	C	D	E	F	G	H	I	J	K	L	M	N
169						283		-6	10	101	466.770318	216.381	16	2.33522
170						283		-6	0	117	480.461538	243.516	6	2.38653
171						283		-6	0	102	480.461538	212.296	6	2.32694
172						283		-6	-25	70	519.520161	134.74	-19	2.1295
173						283		-6	-25	62	519.520161	119.341	-19	2.07679
174						283		-6	-50	66	567.336323	119.858	-44	2.07867
175						283		-6	-50	61	567.336323	107.52	-44	2.03149
176	#18	1984-13	Grade A #10		Inst Charpy Kid	236		0	-10	31	448.193916	69.1665	-10	1.8399
177						236		0	0	32	433.461538	73.8243	0	1.8682
178						233		0	10	35	419.770318	83.3789	10	1.92106
179						236		0	20	36	407.013652	93.363	20	1.97017
180						236		0	30	41	395.09901	103.771	30	2.01608
181			Grade C #4			217		0	-20	38	445.090909	85.3756	-20	1.93133
182						217		0	0	39	414.461538	94.098	0	1.97356
183						217		0	10	41	400.770318	102.303	10	2.00989
184						217		0	20	43	388.013652	110.821	20	2.04462
185			EH36 #5			437		-60	-75	33	781.227273	42.2412	-15	1.62574
186						437		-60	-60	42	743.605634	56.4816	0	1.75191
187						437		-60	-40	51	700.978541	72.7554	20	1.86187
188						437		-60	-20	62	665.090909	93.2203	40	1.96951
189			36T #6			307		-45	-55	38	602.215596	63.1003	-10	1.80003
190						307		-45	-45	40	580.934211	68.8546	0	1.83793
191						307		-45	-35	35	561.441176	62.3386	10	1.79476
192						307		-45	-25	50	543.520161	91.9929	20	1.96375
193	#19	1971-3	ABS-C	25.4	Kid r3 pt bend	269	-2	-23	-196	14.3	1452.72727	9.84355	-173	0.99315
194						269	-2	-23	-196	17.6	1452.72727	12.1151	-173	1.08333
195						269	-2	-23	-151	14.3	946.02459	15.1159	-128	1.17943
196						269	-2	-23	-148	20	925.216	21.8166	-125	1.33479
197						269	-2	-23	-107	23	716.210843	32.1134	-84	1.50669
198						269	-2	-23	-104	24	704.899408	34.0474	-81	1.53208
199						269	-2	-23	-84	27	638.666667	42.2756	-81	1.62609
200						269	-2	-23	-66	34	594.985386	57.1443	-45	1.75697
201						269	-2	-23	-65	33	587.543269	56.1661	-42	1.74947
202						269	-2	-23	-37	48.4	527.207627	91.8044	-14	1.96286
203						269	-2	-23	-34	46	521.58159	88.1933	-11	1.94544
204			302-B	25.4		386	29	-7	-196	20	1569.72727	12.7411	-189	1.10521
205						386	29	-7	-196	25	1569.72727	15.9263	-189	1.20212
206						386	29	-7	-196	37	1569.72727	23.571	-189	1.37236
207						386	29	-7	-157	20	1107.87069	18.0526	-150	1.25654
208						386	29	-7	-157	25	1107.87069	22.5658	-150	1.35345
209						386	29	-7	-132	27	946.191409	28.5355	-125	1.45536
210						386	29	-7	-132	20	946.191409	21.1374	-125	1.32505
211						386	29	-7	-129	24	930.5625	25.7909	-122	1.41147
212						386	29	-7	-101	27	810.982558	33.2929	-94	1.52235
213						386	29	-7	-98	33	800.44	41.2273	-91	1.61519
214						386	29	-7	-73	34	724.885	46.904	-66	1.67121
215						386	29	-7	-73	36	724.885	52.4221	-66	1.71951
216						386	29	-7	-47	42	664.039823	63.2492	-40	1.80106
217						386	29	-7	-45	42	659.934211	63.8427	-36	1.80375
218						386	29	-7	-18	50	610.811765	81.0583	-11	1.91306
219			HY80	25.4		579	-121	-84	-196	31	1762.72727	17.5884	-112	1.24518
220						579	-121	-84	-196	43	1762.72727	24.394	-112	1.38728
221						579	-121	-84	-196	48	1762.72727	27.2305	-112	1.43506
222						579	-121	-84	-157	53	1300.87069	40.7419	-73	1.61004
223						579	-121	-84	-154	49	1277.88235	38.3447	-70	1.58371
224						579	-121	-84	-132	71	1139.19149	62.3249	-48	1.79466

Table 2 continued.

	A	B	C	D	E	F	G	H	I	J	K	L	M	N
225						579	-121	-84	-129	76	1123.5625	67.842	-45	1.83022
226						579	-121	-84	-115	86	1058.47466	62.3539	-31	1.79486
227						579	-121	-84	-107	89	1026.21084	86.7268	-23	1.93815
228						579	-121	-84	-101	70	1003.98256	69.7223	-17	1.84337
229						579	-121	-84	-96	67	986.810169	67.9093	-12	1.83193
230			A517-F	25.4		814	-22	-40	-196	30	1997.72727	15.0171	-156	1.17659
231						814	-22	-40	-196	32	1997.72727	18.0182	-156	1.20461
232						814	-22	-40	-157	30	1535.67069	19.5329	-117	1.29077
233						814	-22	-40	-154	40	1512.88235	26.4396	-114	1.42225
234						814	-22	-40	-132	44	1374.19149	32.0186	-92	1.50541
235						814	-22	-40	-129	45	1358.5625	33.1232	-89	1.52013
236						814	-22	-40	-101	44	1238.98256	35.513	-61	1.55039
237						814	-22	-40	-101	45	1238.98256	36.3201	-61	1.56015
238						814	-22	-40	-73	40	1152.885	34.6956	-33	1.54027
239						814	-22	-40	-73	42	1152.885	36.4303	-33	1.56146
240						814	-22	-40	-73	51	1152.885	44.2368	-33	1.64578
241						814	-22	-40	-59	59	1118.28505	52.7594	-19	1.7223
242						814	-22	-40	-59	63	1118.28505	56.3363	-19	1.75079
243						814	-22	-40	-59	69	1118.28505	61.7016	-19	1.7903
244						814	-22	-40	-45	66	1087.93421	62.5038	-5	1.79591
245						814	-22	-40	-45	70	1087.93421	64.3421	-5	1.8085
246						814	-22	-40	-45	76	1087.93421	71.6955	-5	1.85549
247			HY130	25.4		945	-93	-118	-196	43	2128.72727	20.1999	-78	1.30535
248						945	-93	-118	-196	51	2128.72727	23.958	-78	1.37945
249						945	-93	-118	-154	75	1643.88235	45.6237	-36	1.65919
250						945	-93	-118	-148	79	1601.216	49.3375	-30	1.69318
251						945	-93	-118	-109	98	1399.98171	70.7152	9	1.84951
252						945	-93	-118	-109	102	1399.98171	72.9581	9	1.86248
253						945	-93	-118	-96	96	1352.61017	72.4525	22	1.86005

Table 3. Results of regression analysis on data from each type of test.

	DT TG (25 lines)	CCA (7 lines)	DCB (2 lines)	K_{Id} (1 line)
Mean Slope	0.016	0.007	0.015	0.004
Standard Deviation	0.005	0.003	0.001	
Min. value	0.006	0.004		
Max. value	0.027	0.012		
Mean Intercept (at T-NDTT = 0°C)	1.854	2.191	2.057	
Standard deviation	0.229	0.132	0.02	
Min. value	1.485	2.035		
Max. value	2.361	2.377		

Legend:

DT TG	*Double Tension Temperature Gradient test*
CCA	*Compact Crack Arrest*
DCB	*Double Cantilever Beam*
K_{Id}	*Plane strain dynamic initiation, bend specimens*

Table 4

Details of data falling on or below the Pellini reference toughness curve.

File number	Thick (mm)	Steel/ Test type	Yield MPa	NDTT °C	FATT °C	slope	intercept
88-11	40	steel F DT/Esso	451	-145	-160	0.013	1.653
86-43	35	Norm DT-TG	338	-50	-79	0.023	1.615
86-43	32	Q&T DT-TG	368	-70	-86	0.017	1.763
86-43	40	CR (C/Mn) DT-TG	363	-85	-92	0.015	1.736
86-43	40	OLAC 1.5 Ni DT-TG	413	-135	-166	0.014	1.786
86-43	40	OLAC 2. Ni DT-TG	445	-145	-165	0.016	1.544
86-44	34	SHT 2.5 Ni DT-TG	452	-110	-104	0.027	1.749
86-44	34	SHT 2.5 Ni TDCB	452	-110	-104	0.014	2.043
86-46	22	CR Q&T 3.5 Ni DT-TG	440	-125	-141	0.015	1.741
86-20	75	SHT-DAC DT/Esso	377	-90	-105	0.026	1.485
83-15	25	Si-Mn DT-TG	394	-70	-96	0.016	2.204
83-15	38	Si-Mn DT-TG	382	-50	-94	0.019	1.973
83-15	32	Cu-Ni DT-TG	401	-110	-139	0.017	1.584
83-15	34	0.35 Ni DT-TG	388	-120	-130	0.009	1.817
83-15	40	Cu-Ni DT-TG	422	-70	-122	0.017	1.85
82-40	250	A533 Esso	488	-25	-3	0.006	2.063

Table 5

Details of data falling well above the Pellini reference toughness curve.

Reference	Thick (mm)	Steel/ Test type	Yield MPa	NDTT °C	FATT °C	slope	intercept
82-40	30	KD32 Esso-TG	314	-35	-14	0.027	1.586
83-7	51	A36 CCA	270	-8	35	0.005	2.27
82-40	25	HT80 CCA	771	-60	-110	0.012	2.377
83-18	35	EH36 MACS Esso-TG	392	-55	-90	0.014	2.267
83-18	38	EH36 MACS Esso-TG	363	-50	-125	0.014	2.361

Table 6

CSA S473 requirements based on the Pellini diagram

Thickness (mm)	Moderate crack arrest		Good crack arrest	
	T-NDTT	no-break temp*.	T-NDTT	no-break temp.
$t \leq 26$	5	T	17	T - 12
$26 < t \leq 38$	15	T - 10	26	T - 21
$38 < t \leq 52$	23	T - 17	33	T - 28
$52 < t$	40	T - 35	49	T - 44

*The no-break temperatures are rounded to give the requirements listed in Table 1.

Table 7

Plane strain crack tolerance for CSA S473 requirements based on Pellini reference toughness curve.

Thickness (mm)	Moderate crack arrest			Good crack arrest		
		Critical a			Critical a	
	T-NDTT °C	0.6 σ_y (mm)	σ_y (mm)	T-NDTT °C	0.6 σ_y (mm)	σ_y (mm)
$t \leq 26$	5	15	6	15	25	8
$26 < t \leq 38$	15	25	8	25	35	12
$38 < t \leq 52$	25	35	12	35	60	20
$52 < t$	40	70	26	50	> 100	45

Table 8

Predicted test temperature for 'good' crack arrest based on design line from K_{ca}/σ_{yd} data. (Eq. 3)

'Good' arrest criterion	T - NDTT	No-break temperature
a = 100 mm	55	T - 50
a = 50	42	T - 37
a = 25	28	T - 23

Table 9

Crack tolerance for steels meeting CSA S473 good arrest requirements based on design line from K_{ca}/σ_{yd} data. (Eq. 3)

Thickness (mm)	T - NDTT °C	Kca MPa√m	Critical crack (a) mm
$t \leq 26$	15	41.2	12.3
$26 < t \leq 38$	25	53.6	20.7
$38 < t \leq 52$	35	69.9	35.3
$52 < t$	TBE		

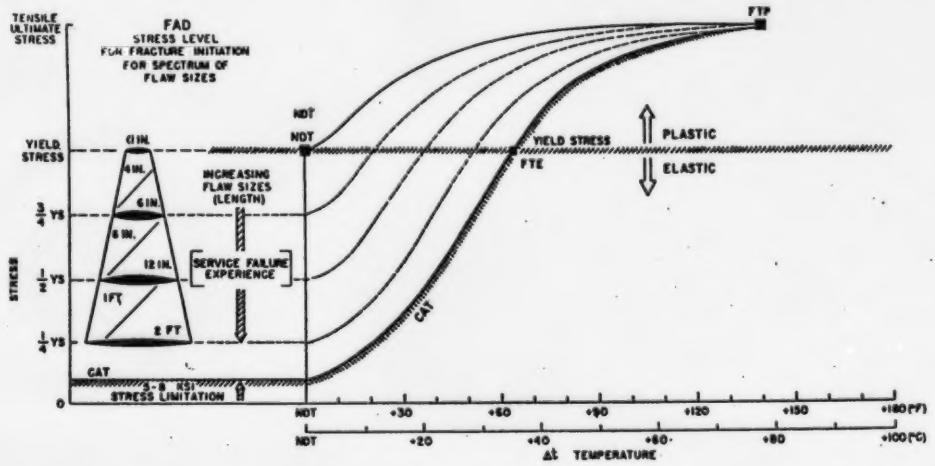

Figure 1. The original Fracture Analysis Diagram (FAD) proposed by Pellini (4). The curve on the right represents crack arrest conditions.

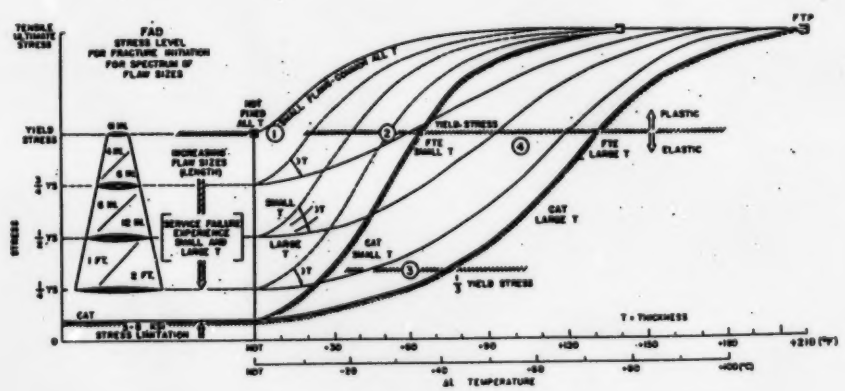

Figure 2. The Fracture Anaysis Diagram (4) revised to include crack arrest curve for thick sections.

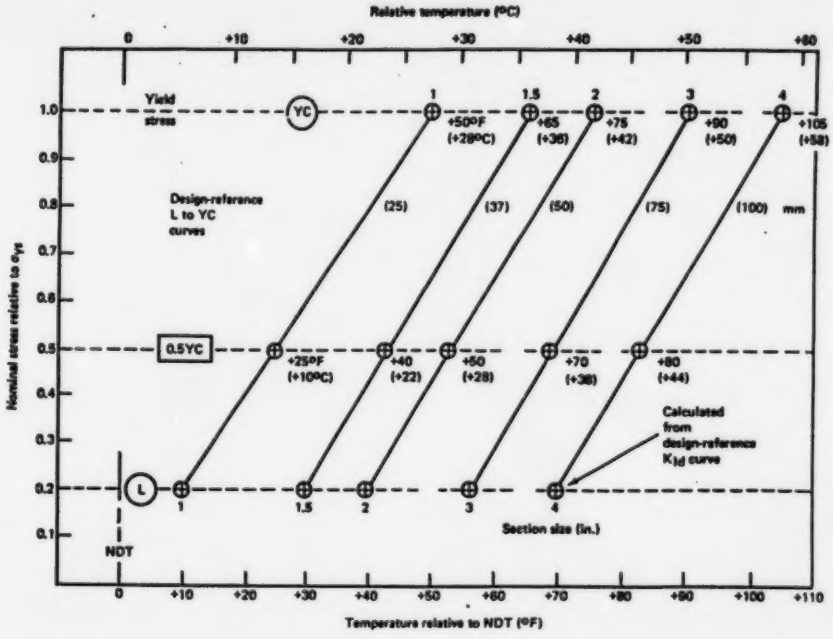

Figure 3. Pellini diagram (6). This version of the Fracture Analysis Diagram uses the *L* and *YC* criteria to establish the crack arrest curve.

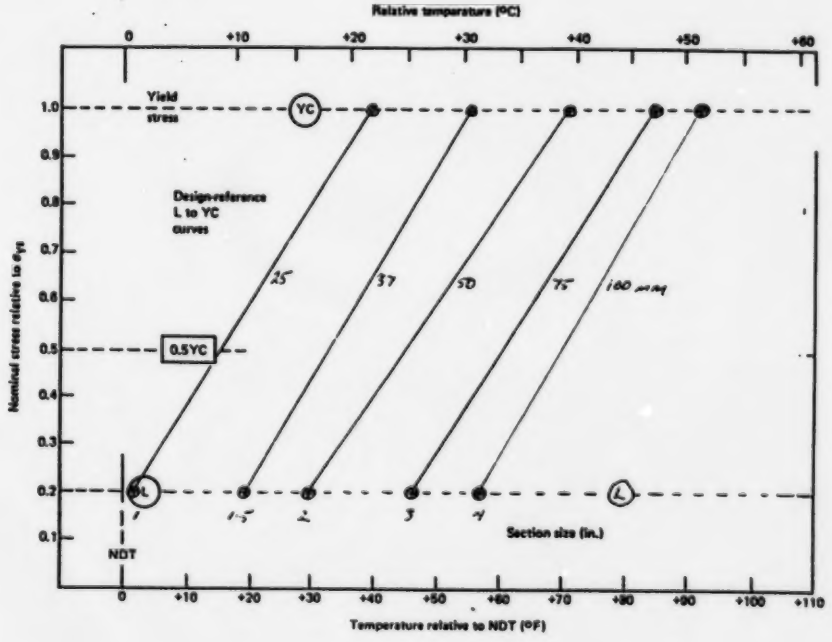

Figure 4. Pellini diagram modified for high dynamic yield stress.

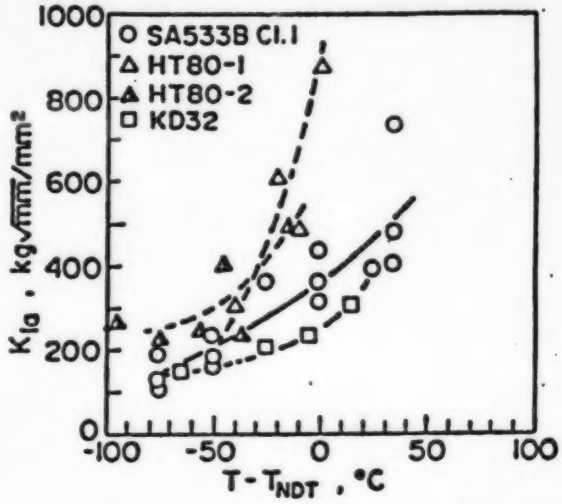

Figure 5. Data from Nakano and Tanaka (15) showing poor correlation between crack arrest toughness and NDTT.

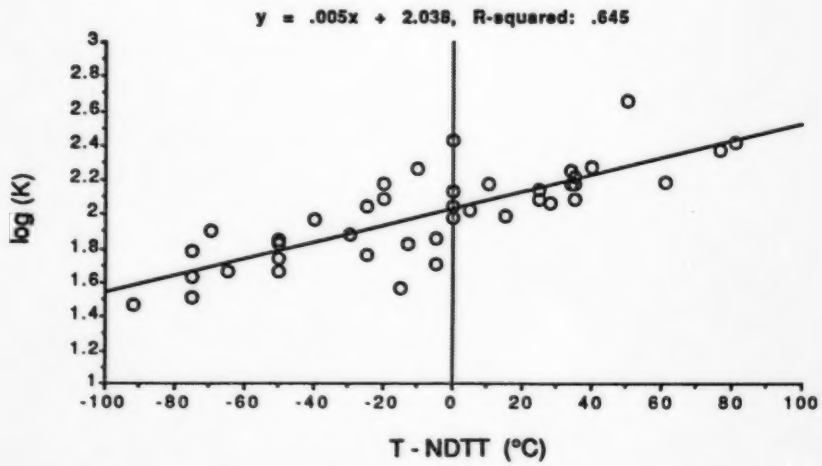

Figure 6. Nakano and Tanaka (15) data plotted in logarithmic form. (Except where otherwise noted, the units of K and σ used in the following graphs are MPa√m and MPa respectively).

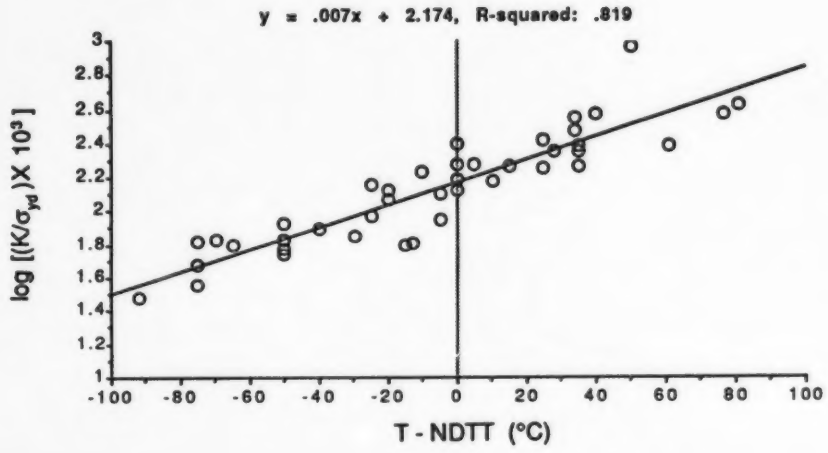

Figure 7. Nakano and Tanaka (15) data plotted in logarithmic form with the toughness normalized with respect to the dynamic yield stress.

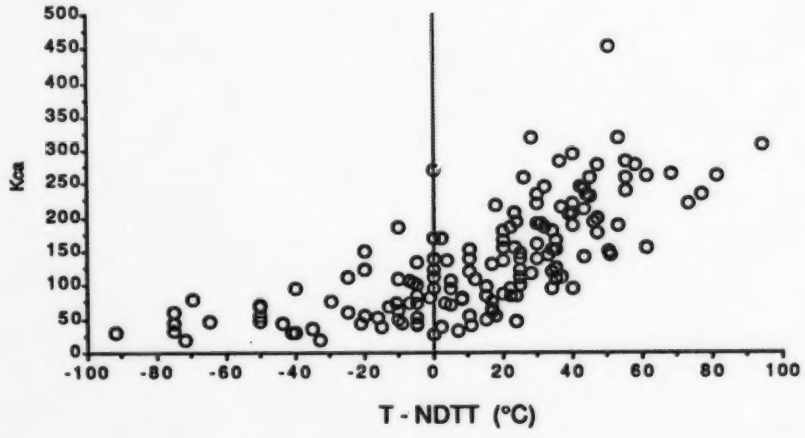

Figure 8. Crack arrest toughness for all results (excluding K_{Id} tests on old steels) plotted against normalized NDTT.

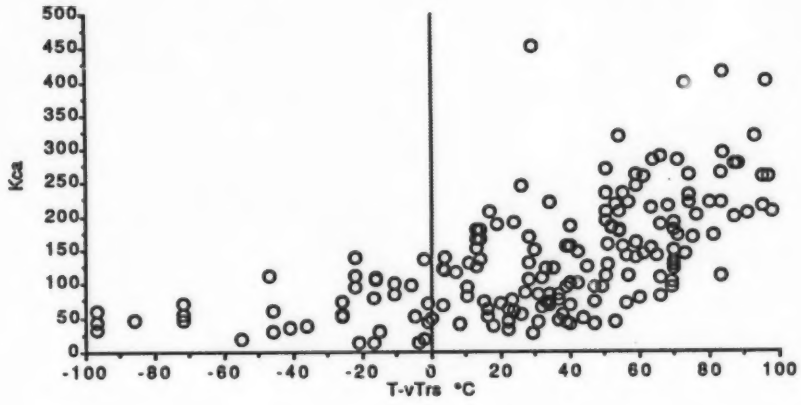

Figure 9. Crack arrest toughness for all results (excluding K_{Id} tests on old steels) plotted against normalized CVN 50% shear transition temperature.

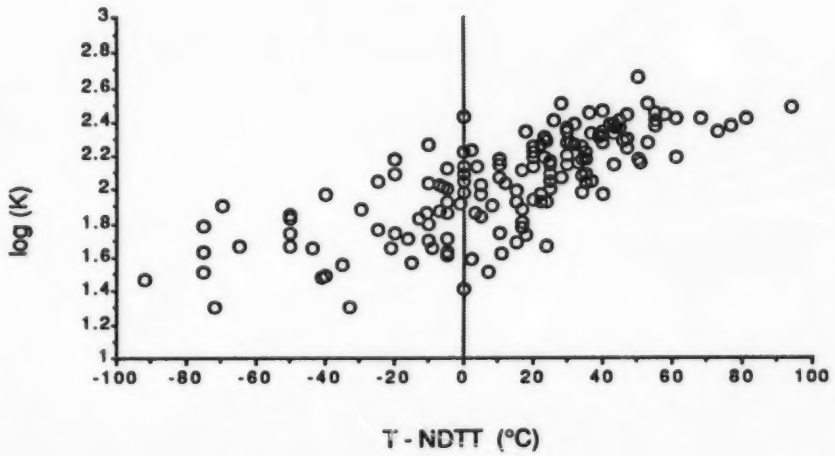

Figure 10. Crack arrest toughness plotted in logarithmic form against normalized NDTT.

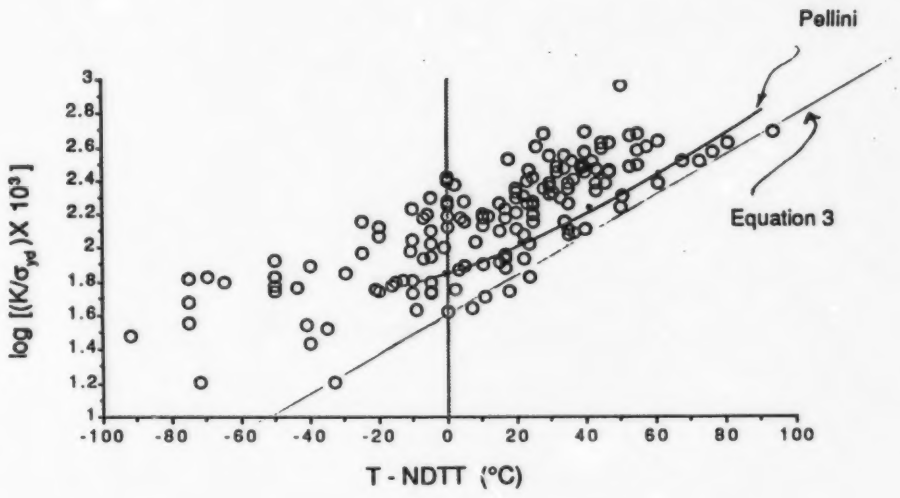

Figure 11. Crack arrest toughness normalized with respect to the dynamic yield stress plotted in logarithmic form against normalized NDTT.

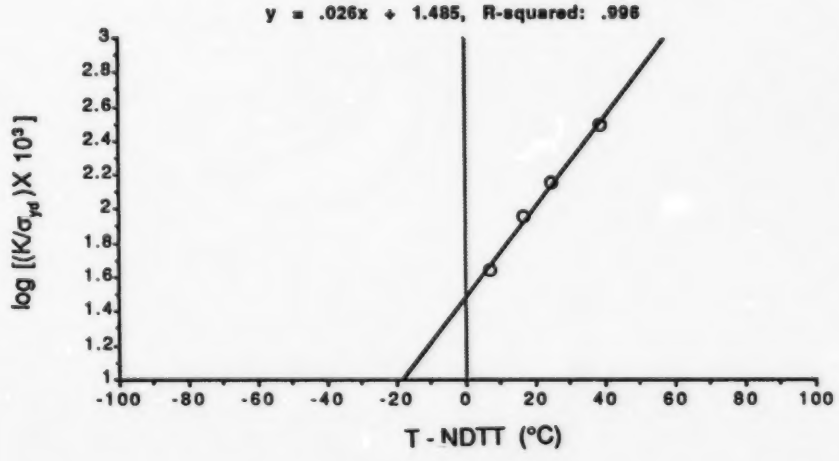

Figure 12. Normalized crack arrest toughness plotted against normalized NDTT for a single steel (12).

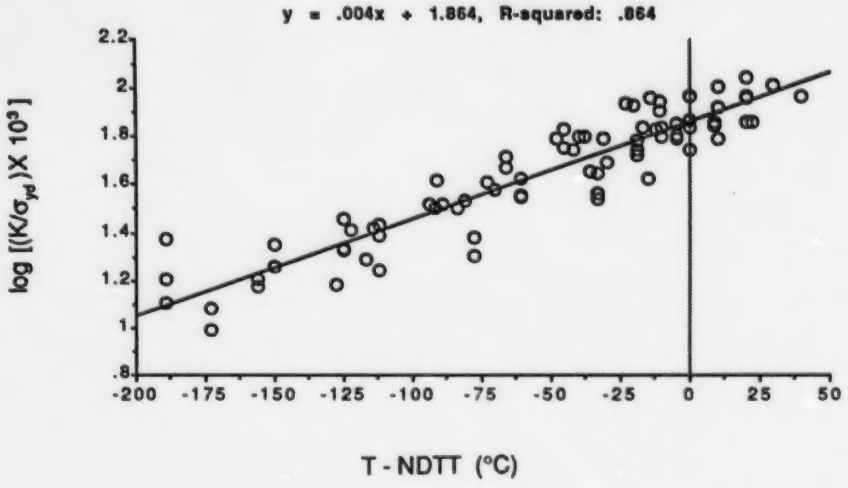

Figure 13. Plot of K_{Id} data in normalized form for older steels. Note the different scale.

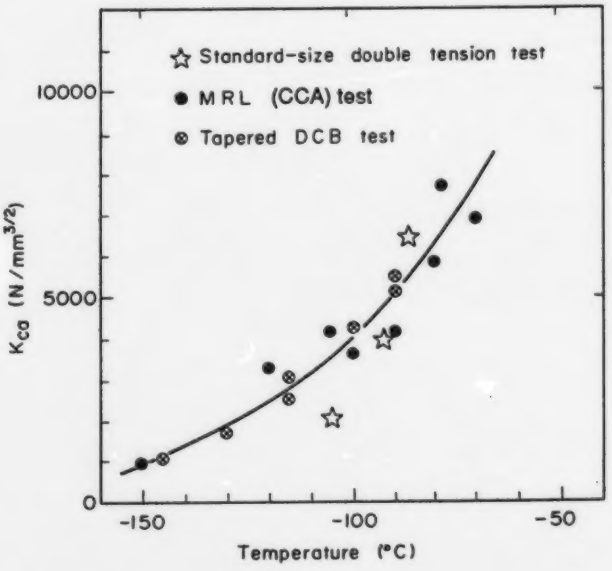

Figure 14. Crack arrest data from various tests on a single steel. The K_{ca} data from double tension tests have a steeper slope and fall below other data around the NDTT.

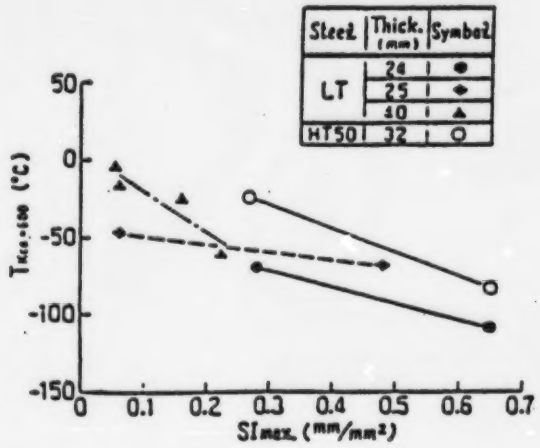

Figure 15. Effect of splitting on crack arrest toughness. Tendency to splitting is represented by the splitting index described in reference 8. Crack arrest toughness is measured by the temperature for a specific value of K_{ca}.

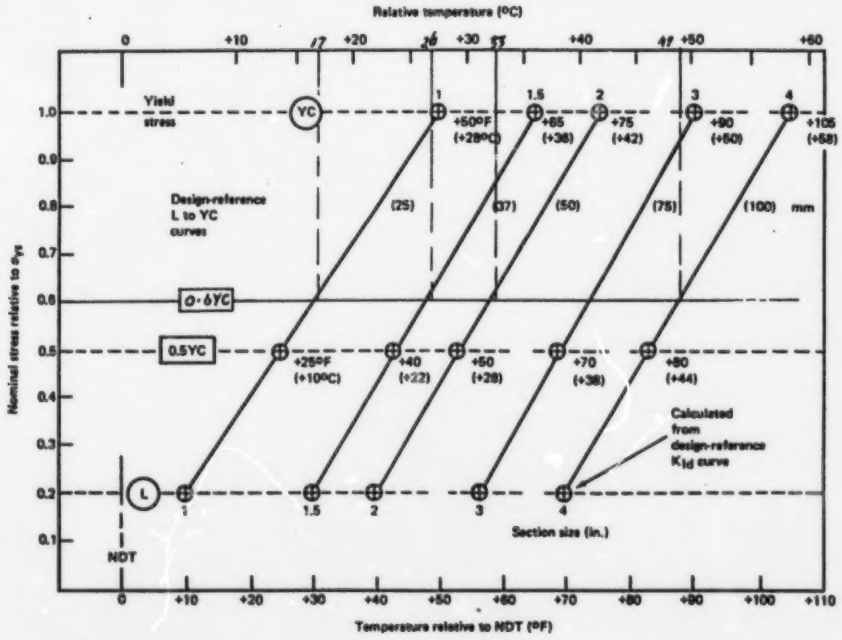

Figure 16. Pellini diagram showing the origin of the CSA S473 requirements.

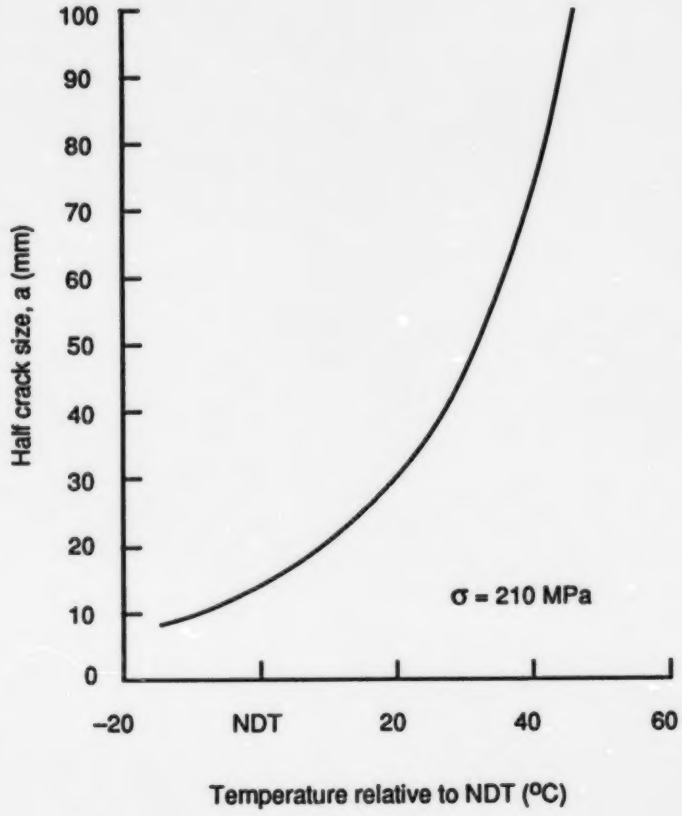

Figure 17. Critical crack size versus temperature relative to NDTT based on Pellini reference toughness curve and a stress of 210 MPa.

Appendix A

Derivation of formula for dynamic yield stress.

Data was taken from the graph (shown on the next page) given in Shoemaker and Rolfe (19) but not including the 18% nickel steels. Regression analysis was performed for three trial relations:

yield strength versus inverse of $T \ln A/\dot{\varepsilon}$
yield strength versus logarithm of $T \ln A/\dot{\varepsilon}$
log yield strength versus log of $T \ln A/\dot{\varepsilon}$.

The first relation gave the best fit with regression coefficients exceeding 0.98.

Regression analysis was then done using this relation for each steel to establish the slopes and intercepts. Using the room temperature yield strength σ_{RT} as an index for each steel, a relation was then sought between the slopes and intercepts and σ_{RT}. Linear relations existed with regression coefficients of 0.99:

$$\text{Slope} = -1.086\sigma_{RT} + 1849.5$$
$$\text{Intercept} = 1.139\,\sigma_{RT} - 232.76$$

Based on the first equation the following relation was tentatively selected:

$$(\sigma_y)_{T,\dot{\varepsilon}} = \sigma_{RT} + \frac{1850 - \sigma_{RT}}{\left[T_{(°K)} \ln\left\langle\frac{A}{\dot{\varepsilon}}\right\rangle\right] \times 10^{-3}} - \text{constant}$$

The best fit of the data to this relation gave the constant as 157. Actual versus predicted values are shown in the figure on the next page. For dynamic loading $\dot{\varepsilon} \sim 10\ s^{-1}$ and Shoemaker and Rolfe give the value $A = 10^8\ s^{-1}$. Thus $\ln A/\dot{\varepsilon} = 16.1$ giving:

$$(\sigma_y)_{T,\dot{\varepsilon}} = \sigma_{RT} + \frac{1850 - \sigma_{RT}}{T_{(°K)} \times 16.1 \times 10^{-3}} - 157$$

Appendix A (cont.)

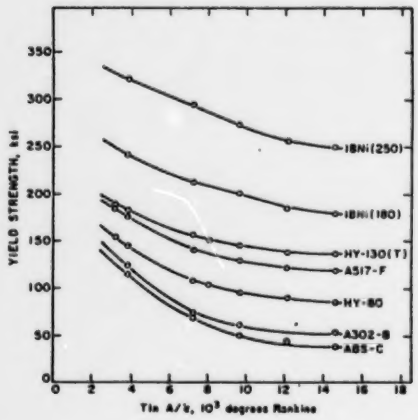

Data from ref. 19 used to derive formula.

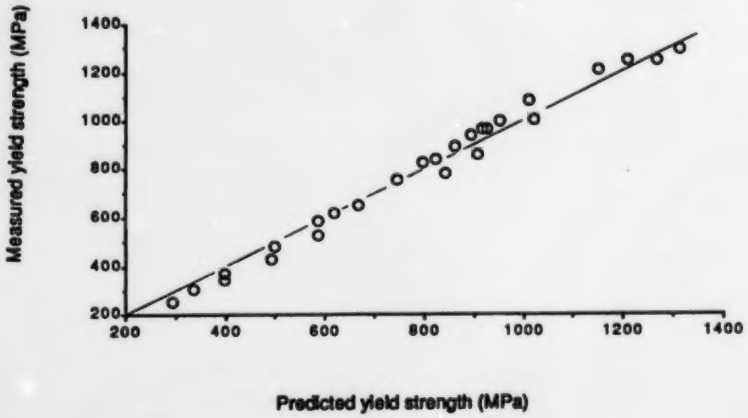

Actual versus predicted values of yield strength.